



# Lawrence Berkeley Laboratory

UNIVERSITY OF CALIFORNIA

## EARTH SCIENCES DIVISION

RECEIVED  
LAWRENCE  
BERKELEY LABORATORY

MAR 26 1985

LIBRARY AND  
DOCUMENTS SECTION

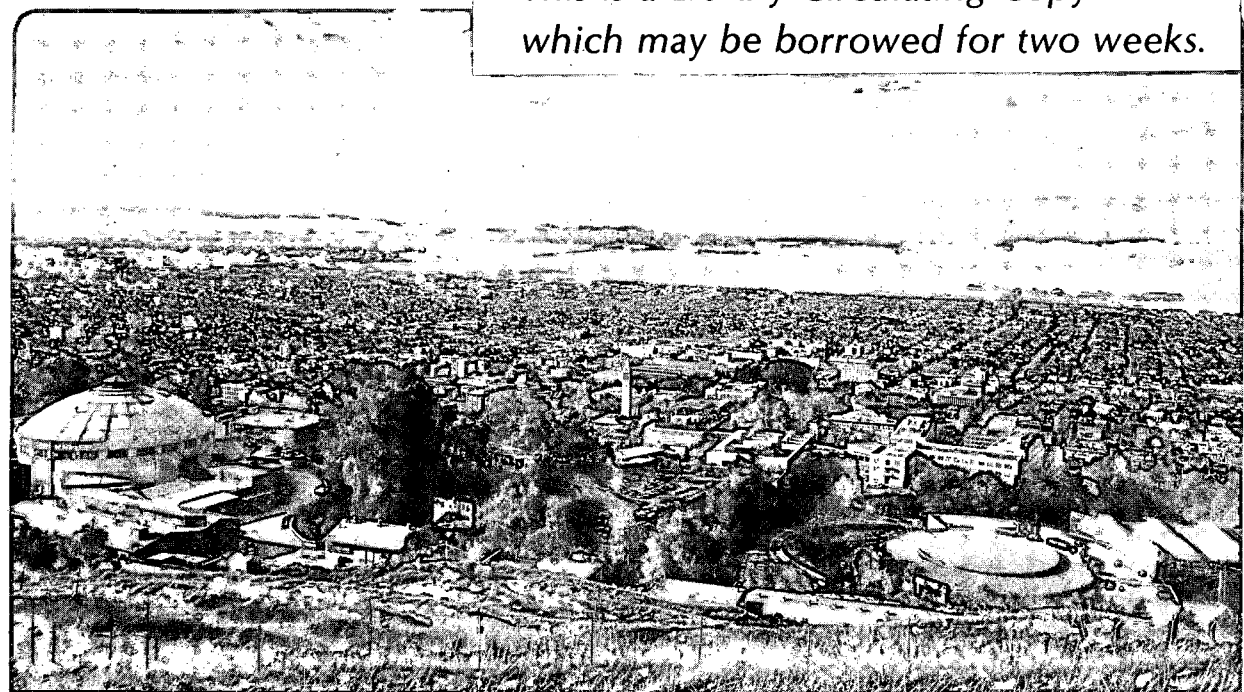
Presented at the 17th International Congress  
International Association of Hydrogeologists,  
Tucson, AZ, January 7-12, 1984

THE EFFECT OF DEFORMABILITY ON FLUID FLOW THROUGH  
A FRACTURED-POROUS MEDIUM

C.F. Tsang, J. Noorishad, and P.A. Witherspoon

October 1984

**TWO-WEEK LOAN COPY**  
*This is a Library Circulating Copy  
which may be borrowed for two weeks.*



LBL-17513  
c.2

## **DISCLAIMER**

This document was prepared as an account of work sponsored by the United States Government. While this document is believed to contain correct information, neither the United States Government nor any agency thereof, nor the Regents of the University of California, nor any of their employees, makes any warranty, express or implied, or assumes any legal responsibility for the accuracy, completeness, or usefulness of any information, apparatus, product, or process disclosed, or represents that its use would not infringe privately owned rights. Reference herein to any specific commercial product, process, or service by its trade name, trademark, manufacturer, or otherwise, does not necessarily constitute or imply its endorsement, recommendation, or favoring by the United States Government or any agency thereof, or the Regents of the University of California. The views and opinions of authors expressed herein do not necessarily state or reflect those of the United States Government or any agency thereof or the Regents of the University of California.

# THE EFFECT OF DEFORMABILITY ON FLUID FLOW THROUGH A FRACTURED-POROUS MEDIUM

Chin-Fu Tsang, J. Noorishad and P. A. Witherspoon  
Earth Sciences Division  
Lawrence Berkeley Laboratory  
University of California  
Berkeley, California 94720

## Abstract

A permeable geologic medium containing interstitial fluids generally undergoes deformation as the fluid pressure changes. Depending on the nature of the medium, the strain ranges from infinitesimal to finite quantities. This response is the result of a coupled hydraulic-mechanical phenomenon which can basically be formulated in the generalized three-dimensional theory of consolidation. In the field of hydrogeology one is concerned with the fluid flow part of this coupled process. Dealing mainly with media of little deformability, traditional hydrogeology accounts for medium deformability as far as it affects the volume of pore spaces, through the introduction of a coefficient of specific storage in the fluid flow equation. This treatment can be justified on the basis of a one-dimensional effective stress law and the assumption of homogeneity of the total stress field throughout the medium. Under such assumptions the changes in permeability that can significantly affect the fluid flow in highly deformable media can be easily dealt with. Quasi-linearized treatment of a combination of one-dimensional consolidation theory and multidimensional fluid flow method is often used.

However, when the homogeneity assumption of the total stress field is no longer valid, one has to resort to more rigorous fully coupled approaches. The inherent anisotropy and inhomogeneity of fractured rocks in regard to both deformational and fluid properties create the need for application of such techniques.

The present paper uses a numerical model called ROCMAS (Noorishad et al., 1982; Noorishad et al., 1984) which was developed to calculate fluid flow through a deformable fractured-porous medium. The code employs the Finite Element Method based on a variational approach. It has been verified against a number of simple analytic solutions. In this work, the code is used to address the role of medium deformability in continuous and pulse testing techniques. The errors that may result because of application of traditional fluid flow methods are discussed. It is found that low pressure continuous well testing or pulse testing procedures can reduce such errors.

## INTRODUCTION

A permeable geologic medium containing interstitial fluids generally undergoes deformation as the fluid pressure changes. Depending on the nature of the medium, the strain ranges from infinitesimal to finite quantities. This response is the result of a coupled hydraulic-mechanical phenomenon. In the field of hydrogeology one is concerned with the fluid flow part of this coupled process. Dealing mainly with media of little deformability, traditional hydrogeology accounts for medium deformability as far as it affects the volume of pore spaces through the introduction of a coefficient of specific storage in the fluid flow equation (Dewist, 1966). This treatment can be justified on the basis of a one-dimensional effective stress law and the assumption of homogeneity of the total stress field throughout the medium. Under such assumptions the changes in permeability that can significantly

affect the fluid flow in highly deformable media can be easily dealt with. Quasi-linearized treatment of a combination of the one-dimensional consolidation theory and multidimensional fluid flow method is often used (Narasimhan, 1977). However, the assumptions are not valid when rapid variations of pressure field are taking place or when the medium possesses strong nonlinearity and anisotropy with regard to different deformation moduli and fluid flow properties (Snow, 1968; Noorishad, 1971; Gale, 1975). In such situations one needs to resort to more rigorous coupled hydromechanical analyses. Development of the general theory of consolidation by Biot (1941) has provided the basis on which more realistic attempts of predicting fluid flow behavior of deformable media have been made. In the following, the numerical code ROCMAS (Noorishad et al., 1982), which was developed on the basis of Biot's formulation, is used to demonstrate the more realistic fluid flow behavior of fractured porous media. It is shown how deformability affects the response of a saturated rock that is subject to injection or pumping. An attempt is made to discuss ways of reducing errors in fractured rock parameter estimation.

#### FIELD EQUATIONS OF COUPLED HYDROMECHANICAL PHENOMENA

Field equations originally formulated by Biot (1941) in his general theory of consolidation form the basis for the hydromechanical analysis of the fractured porous media (Aytollahi et al., 1983). These relationships for the isotropic continuum portions of the medium include the stress-strain equation, the fluid flow law, and the law of static equilibrium which are given as follows:

$$\begin{aligned} \tau_{ij} &= 2\mu e_{ij} + \lambda \delta_{ij} \delta_{kl} e_{kl} + \alpha \delta_{ij} P \\ \zeta &= \alpha \delta_{ij} e_{ij} + \frac{1}{M} P = \alpha e + \frac{1}{M} P \end{aligned} \quad (1)$$

$$\frac{\partial \zeta}{\partial t} = \nabla \cdot \frac{\underline{k}}{\eta_f} \cdot (\nabla p + \rho_f g \nabla z) \quad (2)$$

$$\frac{\partial \tau_{ij}}{\partial x_j} + \rho_s f_i = 0 \quad (3)$$

where

- $\tau_{ij}$  = solid stress tensor
- $e_{ij}$  = solid strain tensor
- $e$  = bulk dilatation equals  $e_{11} + e_{22} + e_{33}$
- $P$  = fluid pressure
- $\delta_{ij}$  = Kronecker delta function
- $\alpha$  = Biot's coupling coefficient
- $M$  = Biot's storativity coefficient
- $\zeta$  = fluid volume strain
- $\underline{k}$  = intrinsic permeability tensor of porous parts
- $\eta_f$  = liquid dynamic viscosity
- $\rho_f$  = fluid mass density
- $\rho_s$  = average porous solid density
- $f_i$  = body force components
- $\mu, \lambda$  = Lamé's elasticity constants

Similarly for the fracture portion of the medium, the corresponding field equations are

$$\begin{aligned} \tau_i &= \delta_{ij} C_{ijk} \bar{U}'_k + \alpha \delta_{i2} P \quad i, j, k = 1, 2 \\ \zeta &= -\alpha \frac{\bar{U}'_2}{2b} + \frac{1}{M} P \end{aligned} \quad (4)$$

$$\frac{\partial \zeta}{\partial t} = \nabla \frac{k}{\eta} (P + \rho_f g z) \quad (5)$$

$$\left. \begin{array}{c} \tau_i \\ \text{US} \end{array} \right| - \left. \begin{array}{c} \tau_i \\ \text{LS} \end{array} \right| = 0 \quad (6)$$

Equation (4) is the stress-strain relationship in which  $\tau_i$  stands for normal and tangential stress;  $C_{jk}$  are the components of fracture moduli (stiffness) matrix,  $\bar{U}_k$  represents the average net tangential or transversal deformation, and  $2b$  is the initial fracture aperture. Coefficient  $\alpha$  and  $M$  are equivalent Biot constants for fractures and  $k$  is the fracture permeability. Equation (5) represents the fracture fluid flow law and Equation (6) balances the forces across the upper and lower faces of the fractures.

The above field equations for the porous solid and the fracture, along with initial and boundary conditions, completely define the mixed initial boundary value problem of fluid flow in deformable fractured porous rocks (Noorishad et al., 1982).

#### SOLUTION APPROACH

The complexity of the phenomenon of fluid flow in deformable fractured rocks make it practically impossible to obtain analytical solutions except for simple problems involving linear isotropic porous media. Extension of the existing variational finite element method for linear elastic porous media (Ghaboussi and Wilson, 1971) by Ayatollahi et al. (1983) and its generalization by Noorishad et al. (1982) provide the numerical formation of the problem as follows:

$$\begin{aligned} \underline{K} \underline{U} + \underline{C} \underline{P} &= \underline{F} \\ \underline{C}^T \underline{U} + \underline{E} \underline{P} + 1^* \underline{H} \underline{P} &= -1^* \underline{Q} \end{aligned} \quad (7)$$

where

- $\underline{K}$  = structural stiffness matrix of the fractured media
- $\underline{C}$  = coupling matrix
- $\underline{E}$  = storativity matrix
- $\underline{H}$  = fluid conductivity matrix
- $\underline{F}$  = nodal force vector
- $\underline{Q}$  = nodal flow vector

In above equation  $\underline{U}$  and  $\underline{P}$  represent the nodal displacement and pressure vectors,  $1^*$  stands for time integration and  $T$  denotes matrix transpose operations.

A predictor corrector scheme is used to obtain the time marching solution of Equation (7). The development of the above equations and the details of the solution are explained in Noorishad et al. (1982). The result is the numerical code ROCMAS, which is used for the computations described below.

#### APPLICATION TO CONTINUOUS FLUID INJECTION PROBLEMS

The problem considered here, as sketched in Figure 1, is that of a horizontal fracture in a low permeability, rigid rock (e.g., granite) located at a depth of 100 meters. A 0.05-m-radius well intersects the fracture at its center. It is assumed that the fracture encounters a region of high permeability capable of maintaining a constant head at a radial distance of 150 m from the well. The rock has a density of  $2600 \text{ kg/m}^3$ . The hydrologic system is at ground level hydrostatic equilibrium before fluid injection takes place. Other system properties are shown in Table 1. To simulate this problem by a two-dimensional model certain assumptions have to be made. The overburden is replaced by

a 10 m slab of rock with a load on its upper surface equal to the remaining 90 m of overburden. Due to the very small deformations involved not much accuracy is lost by ignoring the tangential tractions which might be mobilized at the top of the modeled slab. To ensure static equilibrium, corresponding in situ stress and initial pressures are input into the model. The problem is assumed to have axial symmetry, and its outer boundary is restricted to vertical movement only. The fracture is modeled by a joint element (Goodman et al., 1968) with initial stiffness of  $K_s = 0.5$  GPa/m,  $K_n = 1.6$  GPa/m and assumed to have a linear behavior in the load-deformation range under consideration. To represent the rock rigidity, the Young's modulus is assumed to have a value of 70 GPa. The rock is of sufficiently low permeability ( $10^{-20}$  m<sup>2</sup>), such that under the hydraulic conditions and the time periods considered the flow into the rock itself would be confined to the 10 m slab of the model.

#### Constant Head Injection

Steady state analysis: The system is pressurized by injection under 50 m of constant differential head. Note that the injection head is less than one quarter of the overburden stress on the fracture. The calculated steady state pressure profile in the fracture is plotted in Figure 2. The resulting steady state flow rate is 0.381 m<sup>3</sup>/sec.

Table 1. Data Used for Various Analyses of Fracture Injection Problem.

Material	Property	Problem 1, 3	Problem 2
Fluid	Mass density, $\rho_f$	$9.80 \times 10^2$ kg/m <sup>3</sup>	$9.8 \times 10^2$ kg/m <sup>3</sup>
	Compressibility, $\beta_p$	$5.13 \times 10^{-1}$ GPa <sup>-1</sup>	$5.13 \times 10^{-1}$ GPa <sup>-1</sup>
	Dynamic viscosity, $\eta_f$	$2.80 \times 10^{-4}$ N-sec/m <sup>2</sup>	$2.8 \times 10^{-4}$ N-sec/m <sup>2</sup>
Rock	Young's modulus, $E_s$	70.0 GPa, 0.7 GPa	2.45 GPa
	Poisson's ratio, $\nu_s$	0.25	0.25
	Mass density, $\rho_s$	$2.5 \times 10^3$ kg/m <sup>3</sup>	$2.45 \times 10^3$ kg/m <sup>3</sup>
	Porosity, $c$	0.15	0.15
	Intrinsic Permeability, $k$	$10^{-20}$ m <sup>2</sup>	$10^{-12}$ m <sup>2</sup>
	Biot's constant, * M	1.47 GPa, 14.0 GPa	1.47 GPa 14.0 GPa
	Biot's coupling constant, $\alpha$	1.0, 0.0*	1.0 0.0
	Fractures	Initial normal stiffness, $K_n$	1.60 GPa/m
Initial tangential stiffness, $K_s$		0.50 GPa/m	0.50 GPa/m
Cohesion, $C_0$		0.0	0.0
Friction angle, $\delta$		30°	30°
Initial aperture, ** b		$10^{-4}$ m	$1 \times 10^{-3}$ - $1 \times 10^{-4}$ m
Porosity, $c$		0.50	0.15
Biot's constant, * M		1.47 GPa, 14.0 GPa	1.47 GPa 14.0 GPa
Biot's constant, $\alpha$		1.0, 0.0	1.0 0.0

\* In this case M is the reciprocal of the specific coefficient of storage of the porous medium.

\*\* At every stage of computation calculated fracture apertures of the preceding interactions determine fracture permeability.

In a second set of computations, the calculated flow rate is used to simulate a constant flow rate injection problem. The results of this run plot precisely on the pressure profile curve of Figure 2 as expected, thus adding confidence to the soundness of the steady-state algorithm.

Transient analysis: To simulate the transient behavior of the system in the above problem, the coupled finite element technique (Noorished et al., 1982) is used. The resulting values of the well flow rates are plotted in Figure 3. The curve exhibits an initial exponential decline lasting about 10 seconds followed by a slow rise continuing for about 1000 seconds until a steady state trend of much longer duration takes over. The early time behavior follows the familiar pattern of the constant injection head fluid flow problem. To delineate this behavior, comparison needs to be made between fluid flow equations of the coupled (hydromechanical) problem and that of the equivalent non-deformable problem. In the coupled theory, the flow equation as expressed in Equation (2) or Equation (6) is of the following form:

$$\nabla \cdot \underline{k} \cdot \nabla (P + \rho_f g z) = \frac{\partial}{\partial t} (-\alpha e + \frac{P}{M}) \quad (8)$$

Assuming solid grains are incompressible, the Biot coefficient  $M$  can be replaced by inverse products of porosity  $\epsilon$  and fluid compressibility  $\beta_p$ , resulting in the following representation of the above equation:

$$\nabla \cdot \underline{k} \cdot \nabla (P + \rho_f g z) = \frac{\partial}{\partial t} (-\alpha e + \epsilon \beta_p P) \quad (9)$$

Under the condition of uniform total stresses in the fluid flow region, such as those assumed in the one dimensional theory of consolidation, it is possible to write:

$$\tau' = -P \quad (10)$$

where  $\tau'$  is the effective normal stress in the fracture. Using the definition of compressibility one easily finds

$$\beta_r = -e/P. \quad (11)$$

Notice that  $\tau'$ ,  $P$  and  $e$  are incremental in nature and represent deviations from the initial state. Therefore, using  $e$  from Equation (11) in Equation (9) yields

$$\nabla \cdot \underline{k} \cdot \nabla P = \frac{\partial}{\partial t} (\beta_r + \epsilon \beta_p) P \quad (12)$$

which is the same as the familiar fluid flow equation with  $(\beta_r + \epsilon \beta_p)$  representing the constant specific storage parameter  $S_g$ . Thus, under these conditions, the fluid flow behavior of a deformable porous elastic continuum may be compared with uncoupled fluid flow analysis, based on conventional fluid flow equation. The traditional approach has also been employed for analysis of fluid flow behavior of nonlinear material, such as fractured rocks, by using an equivalent specific storage for fractures defined as  $S_g^f = 1/(2bK_n)$  (e.g. Snow, 1968). Such extensions of the concept of specific storage may be valid only for extensively fractured rocks with frictionless fractures. However, the combination of anisotropy and nonlinearity normally associated with fractures and the consequent pressure-coupled total stress field invalidate such an approach to fluid flow problems in most fractured rocks. To demonstrate this point, the problem under consideration is solved in an uncoupled manner (i.e., fluid flow analysis alone) using an equivalent storage value of  $S_g^f = 1/(2bK_n) = 0.06 \text{ MPa}^{-1}$  (neglecting the much, much smaller fluid compressibility contribution). The results, checked also with Jacob-Lohman's (1951) analytic solution, are much higher than the coupled analysis curve, indicating the need for a much smaller specific storage value in the uncoupled analysis. With some trial and error, using a specific storage of  $2.0 \text{ GPa}^{-1}$ , an uncoupled solution, closely reproducing the coupled curve, is obtained (Fig. 3, Curve C). These investigations point to the fact

that although the fracture tends to behave like an equivalent porous material in regard to fluid flow in the very early period, its storage is not represented by  $1/(2b \cdot K_n)$ , but rather by the overall deformation behavior of the rock-fracture system. This porous medium-like behavior is rapidly violated in later time by the effects of deformation on the intrinsic fracture permeability, necessitating a coupled stress-flow analysis of such problems. Consequently, the early behavior of the coupled results (Fig. 3, Curve B) displaying the same general pattern as the simple fluid flow solution can only be attributed to the fact that fracture permeability does not change much during the early period. However, as the pressure front expands into the fracture, the rock deforms. The increase in flow due to fracture deformation counteracts the normal transient flow decrease. These two effects are balanced at about 10 seconds, after which the fracture deformation effect dominates until the pressure front reaches the boundary and steady flow is achieved. This part of the transient flow rate behavior, which is exaggerated in the log scale, lasts almost 1000 seconds. Final steady state behavior of the model is marked by a small but consistent oscillation about a constant value of about  $0.381 \times 10^{-3} \text{ m}^3/\text{sec}$ . The steady state flow rate obtained earlier closely approximates the fluid results of the transient analysis.

The above transient analysis has been repeated for a much softer rock, with Young's modulus of 0.7 GPa. The same general behavior, though much less striking, is shown in Figure 3, Curve A.

#### Constant flow rate injection

A transient wellbore pressure analysis for a constant flow rate injection test has been made using the same system geometries as described above for the constant head case. The analyses are made using a flow rate of  $0.381 \times 10^{-3} \text{ m}^3/\text{sec}$ , and both deformable and non-deformable conditions are applied for the fracture. In the latter case, a storage coefficient of  $2.0 \text{ GPa}^{-1}$  (as in the earlier problem) is used. The transient pressure curves are shown in Figure 4. As with the transient flow rate case, the results of the conventional fluid flow and the coupled stress and fluid flow analysis follow the same pattern for the very early behavior but deviate as the pressure front advances radially in the fracture. In the deformable fracture, the increase in permeability with time is accompanied by decreasing wellbore pressure until steady flow is finally reached.

#### APPLICATION TO CONTINUOUS PUMPING PROBLEM

In this example an axisymmetric reservoir around a pumping well is assumed with a horizontal fracture at a depth of 320 m. Fluid is assumed to be confined in this aquifer at a piezometric head of 160 m. The aquifer depth and the piezometric head define the geostatic in situ stress distribution and the initial pressure in the aquifer. Therefore, the initial pressure distribution at every point of the aquifer is approximately  $P_0 = (1.5 - 0.01z) \text{ MPa}$ , and the initial stress distribution is  $(8 - 0.025z) \text{ MPa}$  for the vertical component and one-third of that for the horizontal components, where  $z$  denotes the elevations measured from the aquifer center and the number 0.025 MPa approximates the overburden pressure per meter of depth. To keep the model in equilibrium in the initial state, in addition to gravity loading, one has to use an upper boundary pressure distribution of about  $0.025(320 - z_{\text{top}}) \text{ MPa}$ , with  $z_{\text{top}}$  denoting the elevation of the top of the aquifer. Calculations of the above values and other inputs used in this analysis are also based on the data given in Table 1.

Figure 5 shows the finite element mesh used to model the aquifer. Due to early-time sensitivity of the response, greater mesh refinement is required near the pumping well and near the fracture end zone. At large radial distances a coarser mesh is adequate and provides a fair degree of accuracy. Flow is assumed to be taken out of the fracture from the pumping well at the symmetry axis.

The following cases of fluid flow problems where the fracture is assumed to be undeformable (uncoupled problems) are analyzed with this mesh. If uniform flux from the aquifer into the fracture is assumed, the case corresponds to an analytic solution derived by Gringarten and Ramey (1974) which can then be used to verify the model as shown in Fig. 6. The agreement is very good. The same problem, with no assumption about the flux, is also solved in two ways. In the first case, an infinite conductivity fracture, simulated by a 1 mm aperture, serves as a large conduit for fluid flow from the aquifer to the well. The results of this case, being more realistic than the case with constant flux, are plotted in Fig. 6. In the second case, the solution for the most realistic case, that of finite fracture conductivity, is considered. The dimensionless plot of pressure and time quantities, as shown in Fig. 6, exhibits quite different behavior from those of the former cases--although late-time behavior follows the same general trend.

Having performed the traditional fluid flow analyses discussed above, the finite fracture conductivity case is solved in a coupled manner through stress-fluid flow analysis. Figure 7 shows the results of this coupled analysis along with those of the uncoupled analysis taken from Fig. 6. The response is significantly different for the coupled analysis. The increase of effective stresses due to pressure drops caused by fluid withdrawal tends to close the fracture. The degree of closing depends on the fracture compressibility. An average compressibility was used for the fracture in this analysis by assigning 1.6 GPa/m to the fracture stiffness value.

In some practical cases, propping of induced fractures with incompressible grains is normally done. Analysis of such data seems to call for much higher stiffness values and implies justification of the fracture undeformability assumption. However, it is thought that fracture deformability is governed by the degree of compressibility of its void spaces. Therefore, in view of the effect of fracture deformability shown in Fig. 7, controlled experiments for the study of fracture propping in different rock types are necessary.

To provide a better understanding of the fracture deformability effect, the ratio of pressure drop along the fracture over the pressure drop in the well at different relative distances from the well are plotted in Figure 8. The pronounced effect of the fracture deformability is observed in comparison to a similar plot for the uncoupled analysis. It may be noted again that the traditional fluid flow equation of groundwater, also used in our uncoupled analysis, accounts to some degree for the medium deformability through the concept of specific storage. Such representation can only be valid for isotropic media under uniform total stress conditions. However, in the problems discussed here, the difference between the coupled and uncoupled analyses are mainly due to the deformability of the fracture and its consequent drastic permeability changes.

#### APPLICATION TO PULSE FLUID INJECTION PROBLEM

Pulse testing is a well-known procedure in hydrogeology that is used to obtain hydraulic properties of tight formations (Bredehoeft, et al. 1980) and fractured rocks (Wang et al., 1977). In the light of the discussed role of rock deformability effects, and the complexity of the coupled modeling which may be required for its analysis, the idea of aquifer testing by short pressure pulses, rather than continued pressurization, becomes very appealing. The reason lies in the fact that in a pulse test the spread of a diminishing pressure front may not be large enough to overcome the rigidity of the rock. If this is true, the deformation will not play a significant role in the fluid flow response of the rocks. To test this idea, the hypothetical model for the first example (Fig. 1 and Table 1) was simulated for a pressure pulse test. The test was performed in both coupled hydromechanical analysis and uncoupled

simple fluid flow analysis. Figure 9 shows results that are superposed on the constant pressure injection response of the same system in which the end of the fracture is assumed to be closed. The initial vertical offsets in all curves are not of any importance because better selection of the rather arbitrary value of the fracture specific storage in the uncoupled analysis (i.e., fluid flow only), can eliminate this difference. As may be observed, there is significant difference in the behavior of the closed boundary system for the constant pressure injection test, as was the case of open far-end boundary system (figure 5). However, the coupled and uncoupled pulses cause very similar behavior of the model. This confirms the observations made earlier that a pressure pulse with magnitude one-fourth that of the overburden pressure, exerted on a .5 m packed-off section of 0.05 m well radius, does not lead to any appreciable deformation in the fracture. The implication is that the in situ hydraulic properties of the fractures can be obtained with the traditional fluid flow pulse testing analysis methods without any concern for deformability effects. This conclusion is significant for hydraulic testing of tight fractured formations.

#### CONCLUSION

The primary conclusion of this work is that pressure dependence of rock permeability due to fracture deformation may have a major effect on the fluid flow behavior of fractured porous systems. In well testing simulations, the inclusion of fracture deformability results in drastic changes in the form of transient flow rate or pressure curves that may invalidate use of conventional well test type curves. The deformation of the fracture depends on the state of the effective stress tensor in the rock rather than the pressure alone. The deformation of the fracture--and the accompanying deviations from nondeformable behavior--occurs when the pressure front from the injection, or depression front from pumping, has advanced some distance from the well.

Furthermore, using an approximate reformulation of the flow equation in the coupled method, an explanation for early-time behavior of the flow rate in the constant head injection problem is presented. An important conclusion of this attempt is that fluid flow analysis of fractured rocks cannot be generally performed by employing the conventional methods which use the concept of specific storage. The concept of fracture specific storage, based on its deformation moduli (Snow, 1968), is not realistic even under favorable conditions.

The secondary conclusion is that traditional fluid flow approaches for well test analysis are most likely to be valid when testing is at low pressure, say, on the order of 10 percent of the overburden (Snow, 1979), or when pressure pulse testing techniques are used.

Mixed and geometrically complex boundary conditions and variable rock properties will certainly alter the detailed behavior of pressure and fluid flow rate presented in this paper. Nonetheless, it is hoped that coupled hydromechanical studies may provide good insight into such rock behavior, and suggest optimal well test methods.

#### ACKNOWLEDGEMENTS

This paper was prepared under the auspices of the Director, Office of Energy Research, Office of Basic Energy Sciences, Division of Engineering, Mathematics and Geosciences of the U.S. Department of Energy under Contract No. DE-AC03-76SF00098.

## REFERENCES

- Ayatollahi, M.S., J. Noorishad and P.A. Witherspoon, 1983, A finite-element method for stress and fluid flow analysis in fractured rock masses, Journal of Engineering Mechanics Div., ASCE, v. 109, no. 1, pp. 1-13.
- Biot, M.A., 1941, General theory of three-dimensional consolidation, Journal Applied Physics, v. 12 pp. 155-164.
- Bredehoeft, J.D. and S.S. Papadopoulos, 1980, A method for determining the hydraulic properties of tight formations, Water Resources Research, v. 16, no. 1, pp. 233-238.
- DeWiest, R., 1966, On the storage coefficient and the equation of groundwater flow, Journal of Geophysical Research, v. 71, pp. 1117-1112.
- Gale, J.E., 1975, A numerical field and laboratory study of flow in rocks with deformable fractures, Ph.D. Thesis, University of California, Berkeley.
- Ghaboussi, J., and E.L. Wilson, 1971, Flow of compressible fluids in porous media, SESM Report No. 72-12, University of California, Berkeley.
- Goodman, R.E., R.L. Taylor and T. Brekke, 1968, A model for the mechanics of jointed rock, Journal of Soil Mechanics and Foundation Division, ASCE, v. 94, no. SM3.
- Gringarten, A.C., and H. J. Ramey, 1974, Unsteady-state pressure distribution created by a well with a single horizontal fracture, partial penetration or restricted entry," SPE Journal, p. 413, August.
- Jacob, C.E., and S. Lohman, 1952, Nonsteady flow to a well of constant drawdown in extensive aquifer, Trans. Am. Geophys. Union, v. 33 no. 4, pp. 559-569.
- Narasimhan, T.N., and P.A. Witherspoon, 1977, Numerical model for saturated-unsaturated flow in deformable porous media, 1. Theory, Water Resources Research, v. 13, no. 3, pp. 657-664.
- Noorishad, J., M.S. Ayatollahi, and P.A. Witherspoon, 1982, Coupled stress and fluid flow analysis of fractured rocks, International Journal of Rock Mechanics and Mining Sciences, v. 19, pp. 185-193.
- Noorishad, J., P.A. Witherspoon and T.L. Brekke, 1971, A method for coupled stress and flow analysis of fractured rock masses, Geotechnical Engineering Publication No. 71-6, University of California, Berkeley.
- Snow, D.T., 1968, Fracture deformation and changes of permeability and storage upon changes of fluid pressure, Quarterly Colorado School of Mines, v. 63, No. 1, p. 201.
- Snow, D.T., 1979, Packer injection test data from sites on fractured rock, Lawrence Berkeley Laboratory, Report LBL-10080.
- Terzaghi, K., 1925, Erdbaumechanik auf Bodenphysikalischer Grundlage, Leipzig, F. Deuticke.
- Wang, J.S., T.N. Narasimhan, C.F. Tsang and P.A. Witherspoon, 1977, Transient flow in tight fractures, in proceedings of International Well-Testing Symposium, October 19-21, 1977, Lawrence Berkeley Laboratory, Report LBL-7027.

## FIGURE CAPTIONS

- Fig. 1. Schematic geometry of the model used in injection problem.
- Fig. 2. Steady state pressure distribution along the fracture for injection at constant head of 50 m and injection rate of  $3.8 \times 10^{-3} \text{ m}^3/\text{sec}$ .
- Fig. 3. Transient well flow rate versus time for (a) deformable fracture overlain by soft rock ( $E = 0.7$  GPa), (b) deformable fracture overlain by rigid rock ( $E = 70$  GPa) and (c) nondeformable fracture.
- Fig. 4. Transient well pressure versus time for (a) nondeformable fracture and (b) deformable fracture overlain by rigid rock ( $E = 70$  GPa).

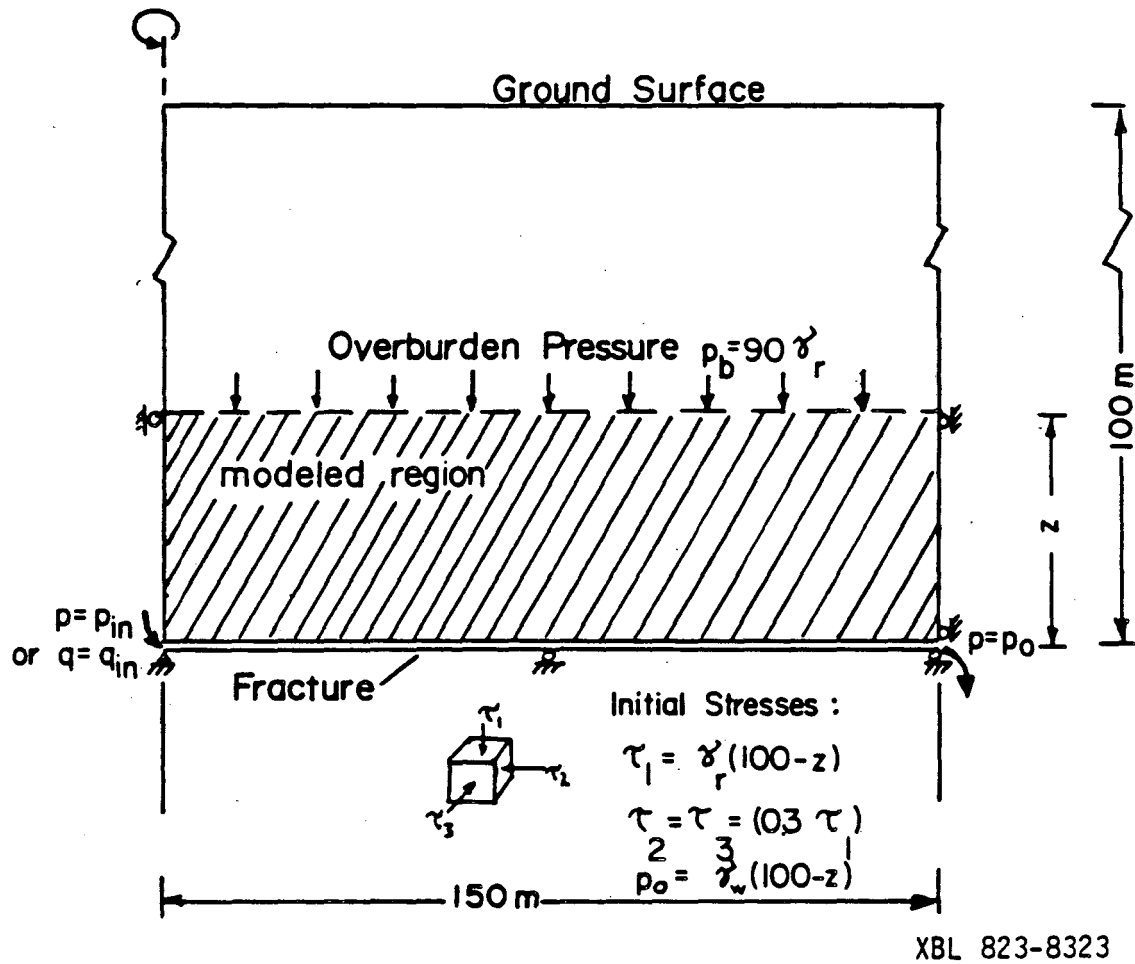
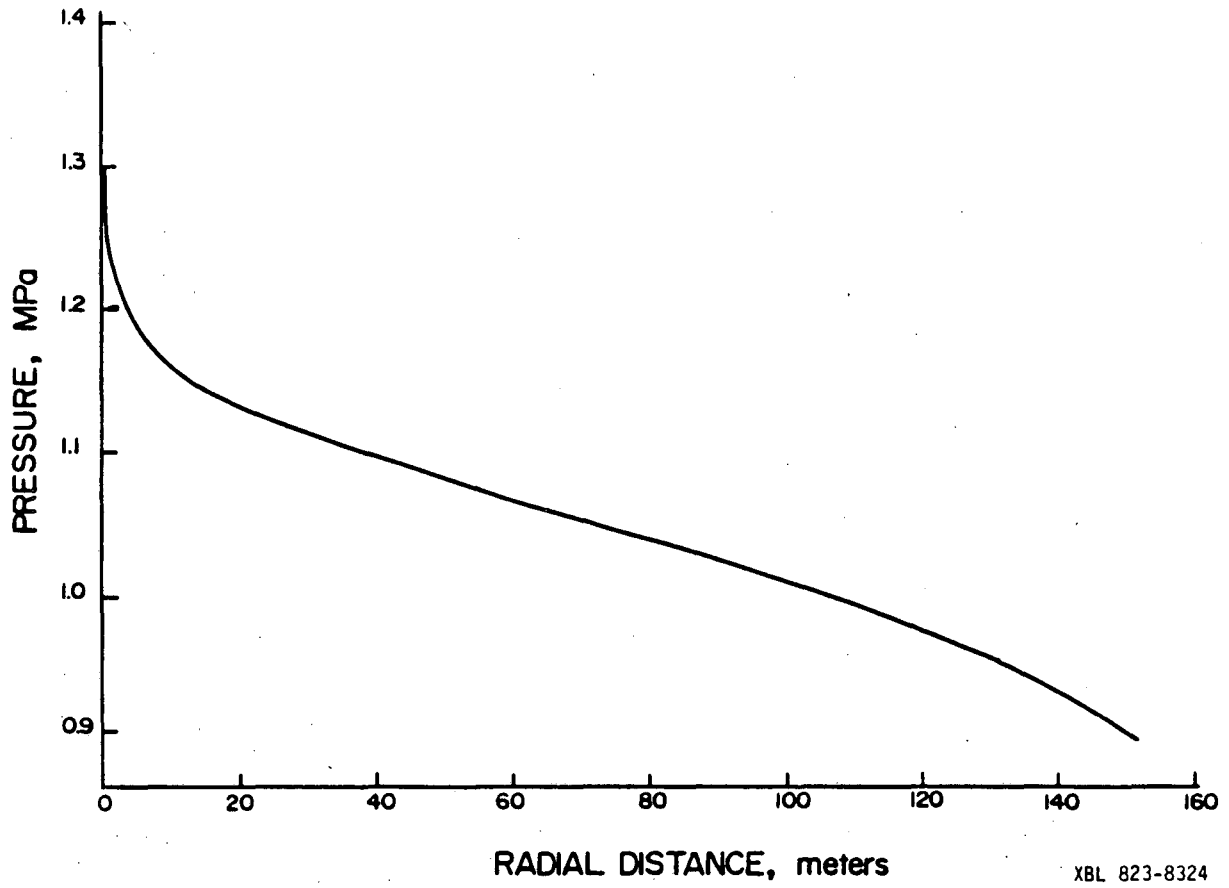
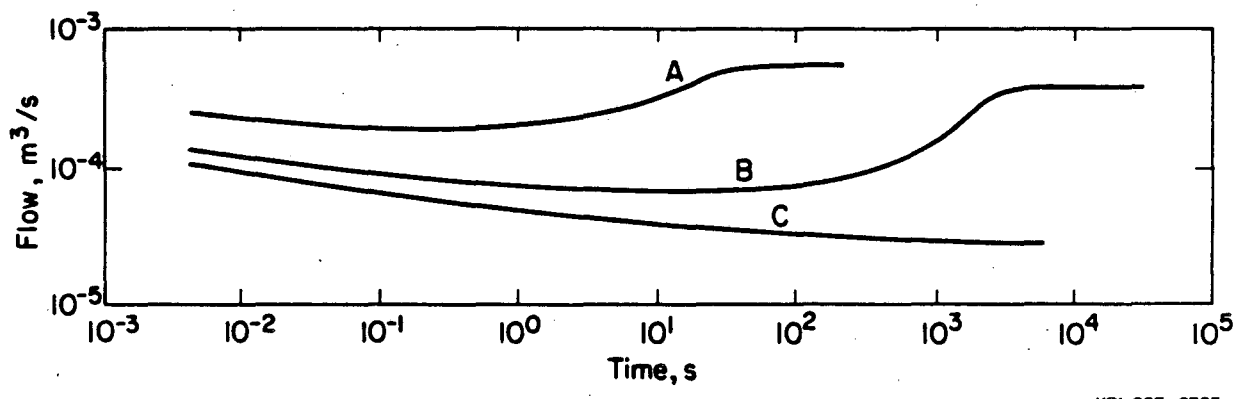


Fig. 1. Schematic geometry of the model used in injection problem.



XBL 823-8324

Fig. 2. Steady state pressure distribution along the fracture for injection at constant head of 50 m and injection rate of  $3.8 \times 10^{-3} \text{ m}^3/\text{sec}$ .



XBL 823-8325

Fig. 3. Transient well flow rate versus time for (a) deformable fracture, (b) deformable fracture overlain by rigid rock ( $E = 7.0 \text{ GPa}$ ) and (c) deformable fracture overlain by soft rock ( $E = 0.7 \text{ GPa}$ ).

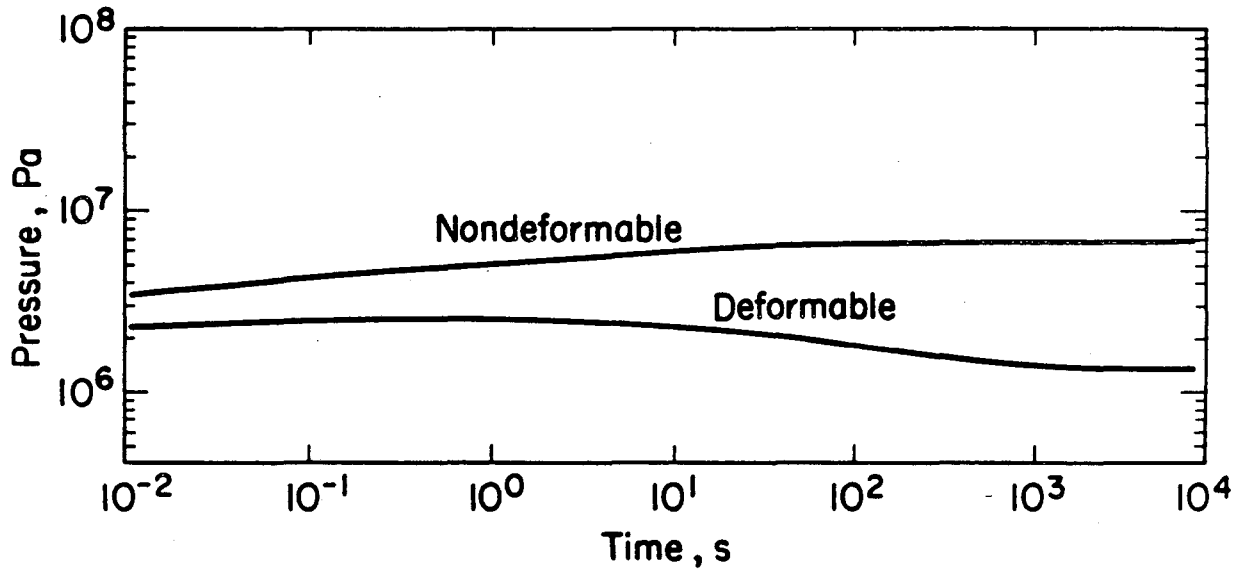


Fig. 4. Transient well pressure versus time for (a) nondeformable fracture and (b) deformable fracture overlain by rigid rock ( $E = 70$ . GPa).

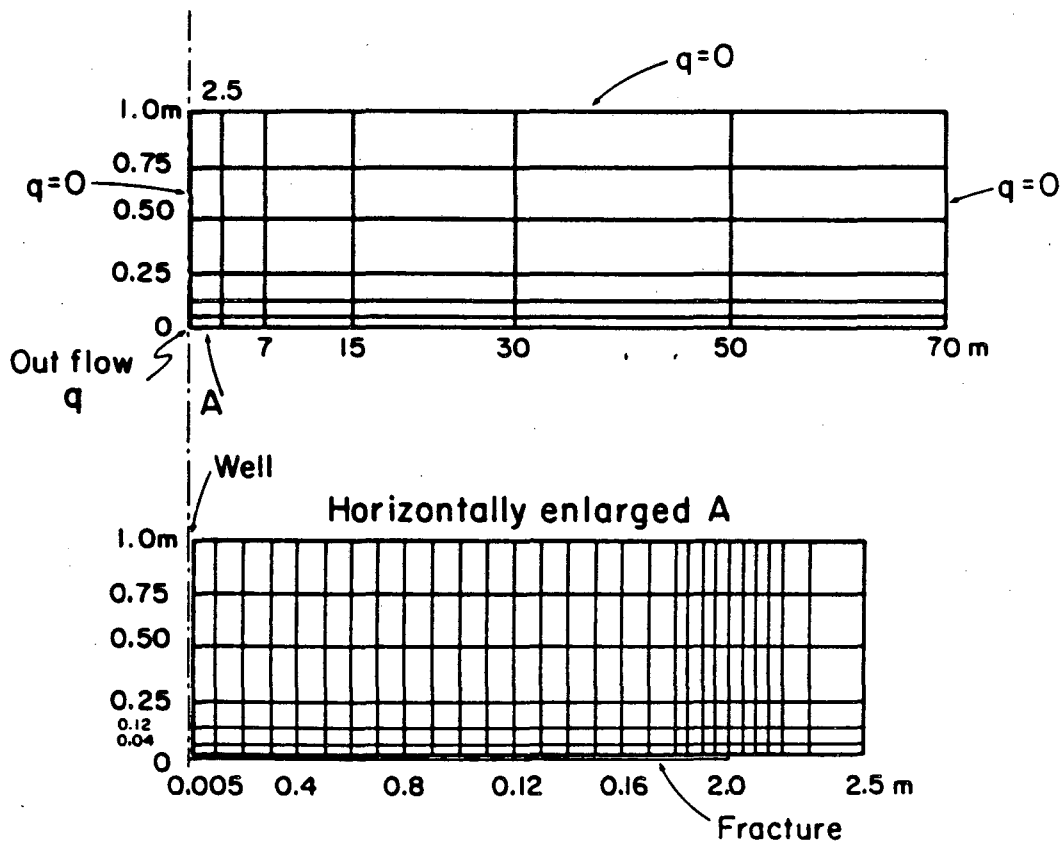
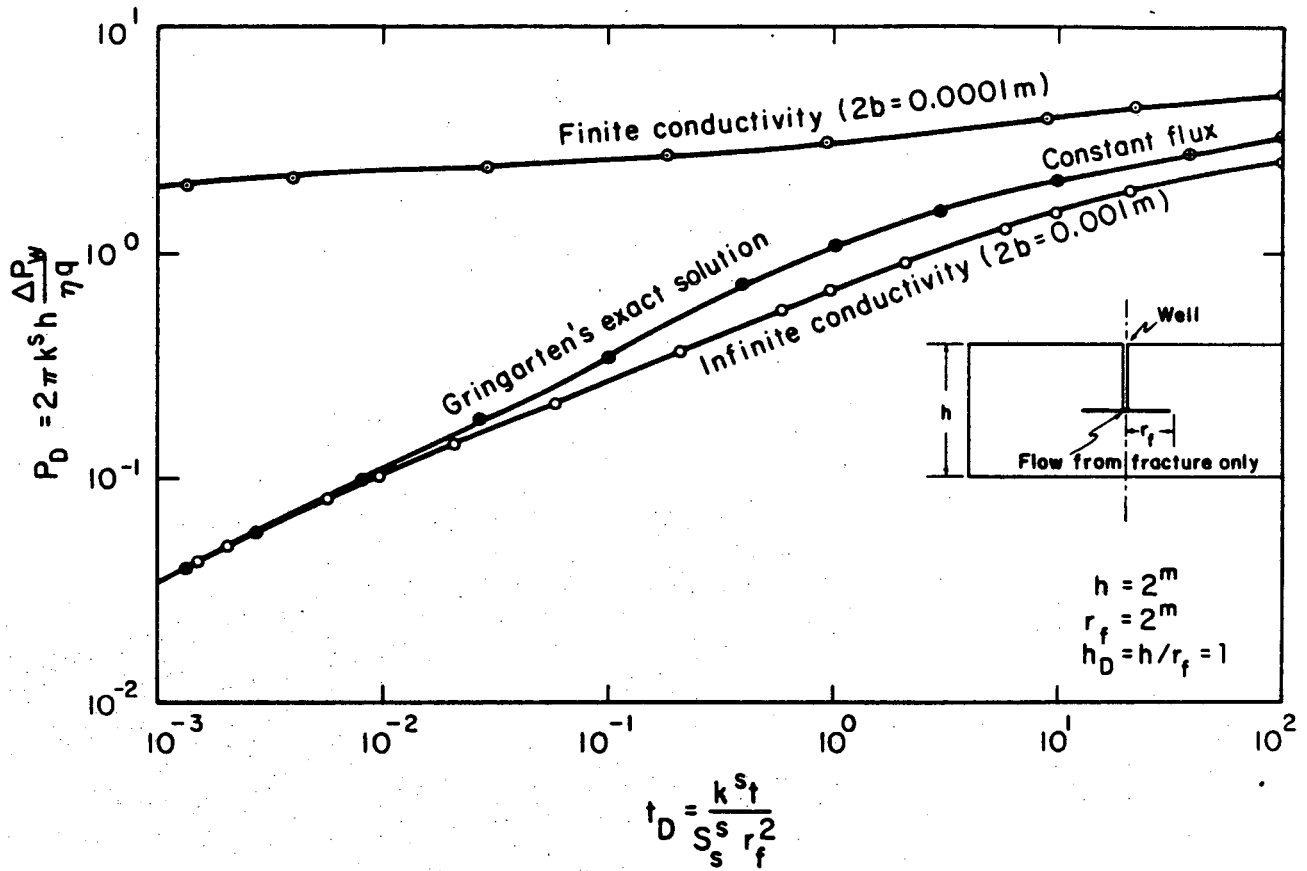
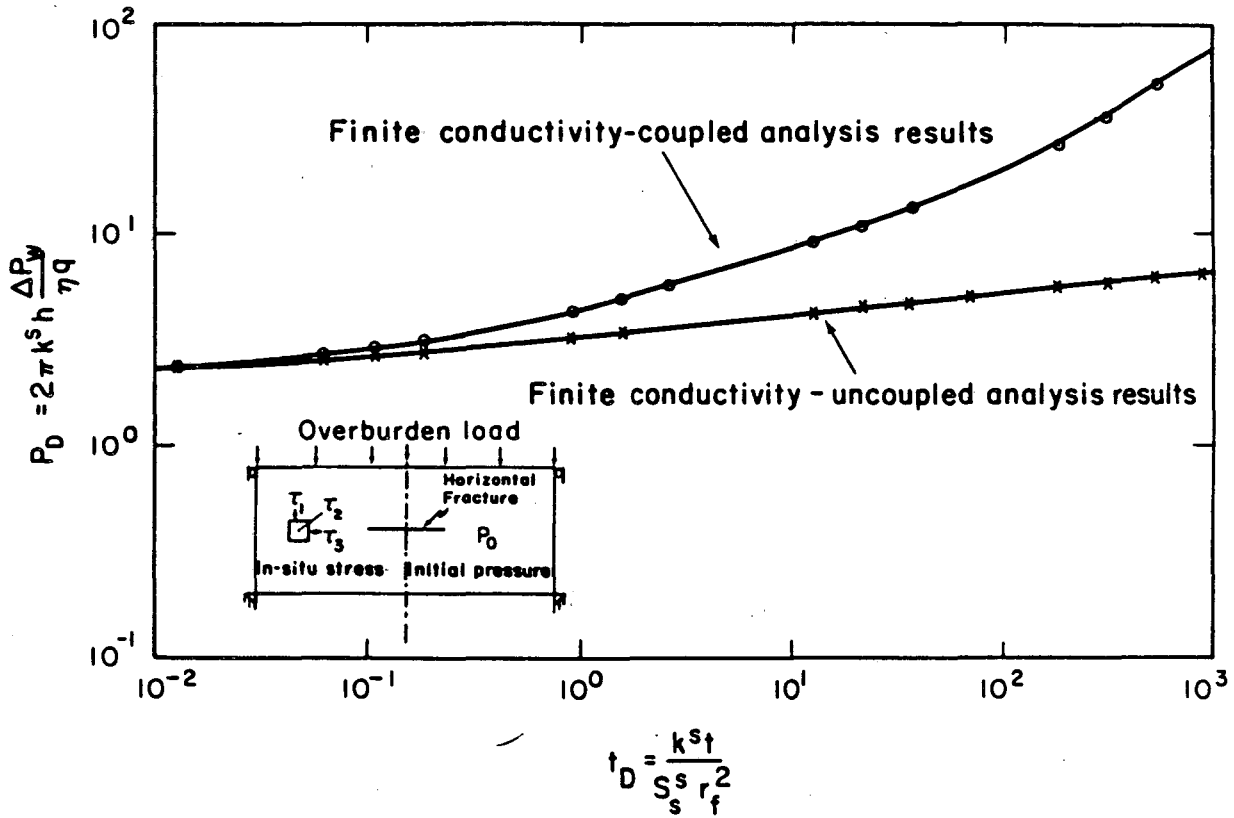


Fig. 5. Axisymmetric finite element mesh.



XBL813-2708

Fig. 6. Dimensionless pressure in well versus dimensionless time for different uncoupled problems.



XBL 813-2709

Fig. 7. Dimensionless pressure in well versus dimensionless in coupled and uncoupled analysis.

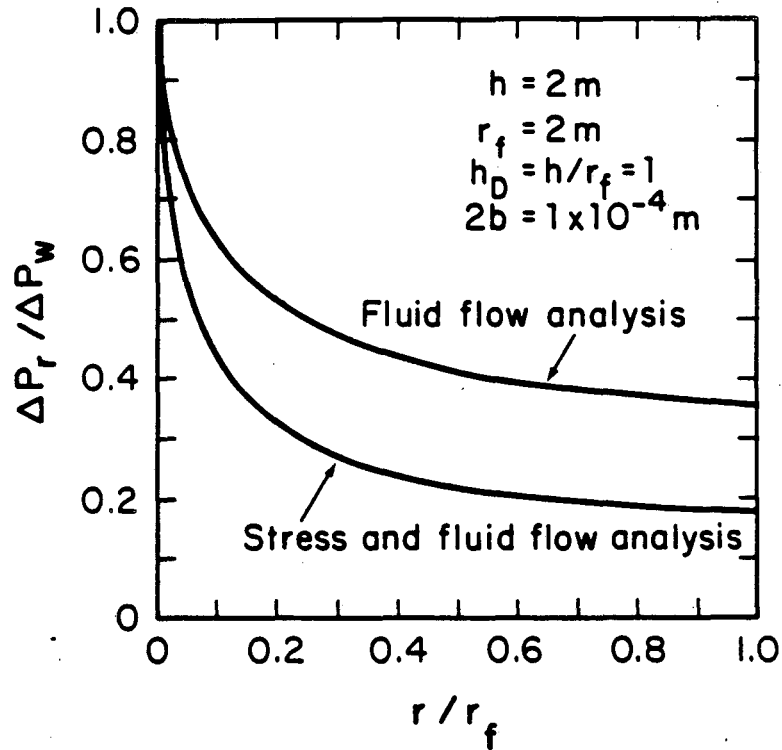


Fig. 8. Pressure drop along the fracture in coupled and uncoupled analysis.

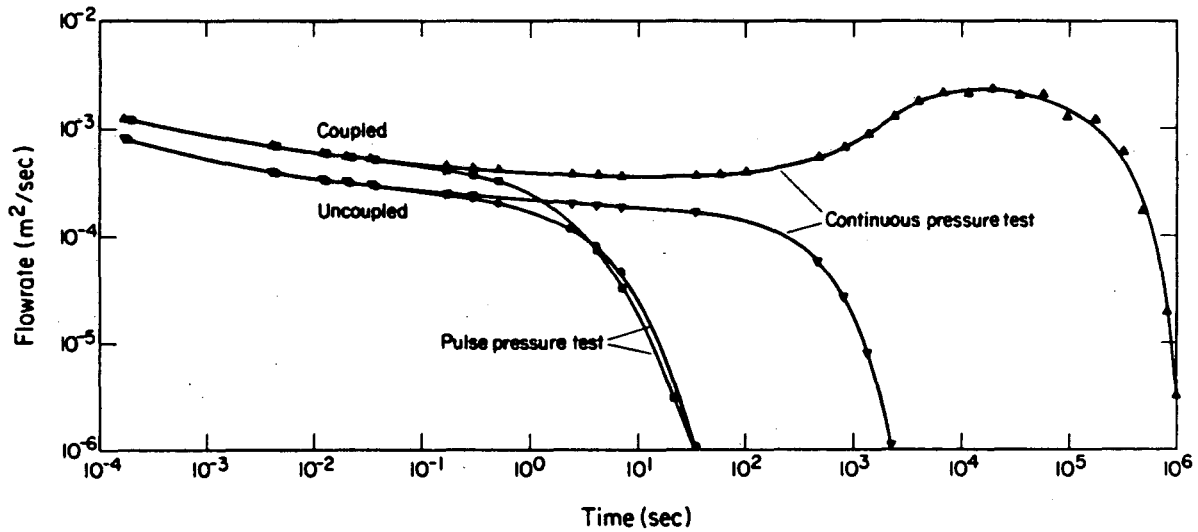


Fig. 9. Transient well flow rate versus time for deformable and undeformable fracture in pulse pressure testing and constant pressure testing.

This report was done with support from the Department of Energy. Any conclusions or opinions expressed in this report represent solely those of the author(s) and not necessarily those of The Regents of the University of California, the Lawrence Berkeley Laboratory or the Department of Energy.

Reference to a company or product name does not imply approval or recommendation of the product by the University of California or the U.S. Department of Energy to the exclusion of others that may be suitable.

TECHNICAL INFORMATION DEPARTMENT  
LAWRENCE BERKELEY LABORATORY  
UNIVERSITY OF CALIFORNIA  
BERKELEY, CALIFORNIA 94720